CSIRO PUBLISHING

RESEARCH PAPER
https://doi.org/10.1071/WF21072

International Journal of WILDLAND FIRE
International Association of Wildland Fire

Reconstructing seasonal fire danger in southeastern Australia using tree rings

Kathryn Allen[A,B,C,*], Stephen B. Stewart[D], Carly Tozer[E], Doug Richardson[E], Craig Nitschke[B], James Risbey[E], Andrew Dowdy[F], Matthew Brookhouse[G], Paul Fox-Hughes[F], Mike Peterson[H] and Patrick J. Baker[B]

For full list of author affiliations and declarations see end of paper

*Correspondence to:
Kathryn Allen
Geography, Planning, Spatial Sciences, University of Tasmania, Sandy Bay, Tas. 7005, Australia
Email: Kathryn.Allen@utas.edu.au

Received: 27 May 2021
Accepted: 11 April 2022
Published: 13 May 2022

Cite this:
Allen K *et al.* (2022)
International Journal of Wildland Fire
31(6), 559–571. doi:10.1071/WF21072

ABSTRACT

Climate projections indicate that dangerous fire weather will become more common over the coming century. We examine the potential of a network of temperature- and moisture-sensitive tree-ring sites in southeastern Australia to reconstruct the number of high fire-danger days for the January–March season. Using the Forest Fire Danger Index (FFDI), we show that modestly statistically skilful reconstructions for the far southeast of Australia (western Tasmania), where the majority of tree-ring predictors are located, can be developed. According to the averaged reconstructions for the 1590–2008 period, there have been 16 years prior to the start of the FFDI records (1950), and 7 years since 1950, with >48 (mean + 1σ) high fire-danger days in the 3-month season. The western Tasmanian reconstructions indicate extended relatively high fire-danger periods in the 1650s–1660s and 1880s–1890s. Fire danger has also been relatively high since 2000 CE. A persistent increase in the number of high fire-danger days over the past four decades has not been matched over the previous 390 years. This work indicates it is possible to produce statistically useful reconstructions of high seasonal fire danger – as opposed to fire occurrence – but that availability of local proxy records is key.

Keywords: climate change, drought factor, Forest Fire Danger Index, paleoproxy fire records, reconstruction, seasonal fire danger, Tasmania, tree rings.

Introduction

The catastrophic devastation (Davey and Sarre 2020) wrought by the 2019–2020 Australian fire season was a brutal reminder of the escalating impacts inflicted on Australia by climate change (van Oldenborgh *et al.* 2021). The 2019–2020 season occurred against a backdrop of severe and prolonged drought, and the hottest year on record in Australia (Abram *et al.* 2021). At the same time, the incidence of dangerous weather conditions that cause intense large-scale fires in the Australian landscape has increased since records have been kept (Dowdy 2018; Harris and Lucas 2019), consistent with the trend direction in projections of fire risk (Reisinger *et al.* 2014; Dowdy *et al.* 2019).

Palaeoproxy fire records indicate considerable variability in fire incidence through time (Power *et al.* 2008; Mooney *et al.* 2011). For Australia generally, relatively high levels of burning occurred ~38 000 years before present (yBP) and from ~35 000–27 000 yBP, followed by low levels of burning during the last glacial maximum (~21 000–16 000 yBP) and around 6000 yBP. The rapid increase in fire incidence over the last two centuries (Mooney *et al.* 2011), however, appears unprecedented in the context of the longer record. There is evidence that long-term global variability in fire occurrence is associated with major climatic fluctuations associated with glacial cycles, and by drivers such as the Southern Annular Mode (SAM) or the El Niño Southern Oscillation (ENSO) (Meyn *et al.* 2010; Mariani and Fletcher 2016; Holz *et al.* 2017).

Significant effort has led to the development of past fire records in many regions, including in Australia (Marsden-Smedley 1998; Mooney *et al.* 2011; Stahle *et al.* 2016), North America (Swetnam 1993; Whitlock et al. 2015), Russia (Ivanova et al. 2010; Kharuk et al. 2016), Asia (Hessl et al. 2011), South America (Holz et al. 2017) and Central America (Cerano-Paredes 2021). Research has also focused considerable attention on developing reconstructions of temperature and hydroclimate (Cook et al. 2010; Williams et al. 2012; Reisinger et al. 2014; Littell et al. 2016; Esper et al. 2018; Chavardès et al. 2019; Morales et al. 2020; Büntgen et al. 2021; Sun et al. 2021), and indices such as ENSO (Trouet et al. 2006; Meyn et al. 2010; Li et al. 2013), which are linked with fire danger. Indices of seasonal fire danger, however, have not typically been a target for reconstructions (but see Chavardès et al. 2020). Although fire incidence and fire weather are linked with factors such as high temperature and drought, they describe distinctly different phenomena (Chavardès et al. 2019, 2020). Human agency and land management practices, for example, have been shown to be important drivers of fire occurrence (Flannigan et al. 2009a; von Platen et al. 2011; Collins et al. 2015; Hanson et al. 2015; Pyne 2016; Fletcher et al. 2020). A reconstruction of a fire-danger index, such as the Forest Fire Danger Index (FFDI) for Australia, would provide a useful complement to reconstructions of related climate variables such as drought and temperature.

The FFDI (McArthur 1967) is a representation of the expected rate of fire spread or suppression difficulty given the combination of its components. It is widely used to indicate dangerous weather conditions for wildfires (commonly referred to as bushfires) in Australia. It is comprised of four components: temperature, relative humidity, a drought factor and wind speed. It can be expressed as:

$$\mathrm{FFDI} = \exp(0.0338\mathrm{T} - 0.0345\mathrm{RH} + 0.0234\mathrm{v} + 0.243147) \times \mathrm{DF}^{0.987}$$

where T is temperature, RH relative humidity, DF a drought factor estimating the proportion of fine fuel available to burn, based on the Keetch–Byram drought index (Keetch and Byram 1968) to reflect soil moisture, and v is wind speed (km/h) (Noble et al. 1980). Although the FFDI has limitations, it has, over the instrumental period, been closely linked with large and/or intense forest fires, particularly in temperate regions of southern and eastern Australia (Dowdy et al. 2009; Abram et al. 2021).

Gridded FFDI data are now available for the 1950–2019 period at high resolution (0.05° × 0.05°) (Dowdy 2018). These are based on gridded analysis of observations as provided by data from the Australian Water Availability Project (Jones et al. 2009). These data provide an opportunity to investigate the possibility of reconstructing Australian seasonal fire danger for years prior to 1950 using proxy records with annual resolution such as tree rings. Tree-ring chronologies in southern Australia are sensitive to temperature, precipitation and drought (Buckley et al. 1997; Cook et al. 2000; Cullen and Grierson 2009; Allen et al. 2015, 2018; Palmer et al. 2015; Nitschke et al. 2017; O'Donnell et al. 2018), all of which are included in the formulation of the FFDI. Temperature and drought, in particular, have been widely implicated as critical fire risk factors (Flannigan et al. 2009a; Meyn et al. 2010; Williams et al. 2014; Abram et al. 2021).

In this study we exploit the drought and temperature sensitivity of various tree-ring chronologies in southeastern Australia to test the potential for reconstructing past fire conditions in the region. Temperature, drought and humidity are all critical elements of seasonal fire danger (Williams et al. 2014; Goss et al. 2020). The importance of wind for influencing fire danger, as represented in indices such as the FFDI or other fire indices (Dowdy et al. 2009), poses an important challenge. However, although wind is important for individual cases of extreme fire danger at daily–weekly scales, variation in fire weather at longer climate time scales in Australia appears to be primarily driven by factors other than wind. These include temperature, relative humidity, rainfall and drought (Dowdy 2018), based both on post-1950 observations and 21st Century climate projections (CSIRO and Bureau of Meteorology 2015). The trees' ability to capture variables that play an important role in long-term variability in fire danger suggests there is merit in testing their ability to capture past fire conditions as encapsulated in the FFDI. Such reconstructions may be especially valuable in helping to understand the extent of the link between seasonal fire danger and fire incidence prior to the 20th Century.

Materials and methods

Tree ring chronologies

The majority of the tree-ring sites used in this study are located in Tasmania, with some additional sites in Victoria (Table 1, Fig. 1). The Tasmanian chronologies are based on four long-lived conifers: Huon pine (*Lagarostrobos franklinii*); King Billy pine (*Athrotaxis selaginoides*); pencil pine (*Athrotaxis cupressoides*); and celery top pine (*Phyllocladus aspleniifolius*). There are also five Victorian tree-ring chronologies. Four of these are based on Melbourne City street trees: oak (*Quercus robur* L.); elm (*Ulmus* spp.); white poplar (*Populus alba*); and one has been developed from snowgum (*Eucalyptus pauciflora*) in the Victorian highlands (Fig. 1). These sites were selected from an existing network and are sensitive to temperature or hydroclimate (Cook et al. 1991; Allen et al. 2001, 2011, 2015, 2017a, 2017b, 2018, 2019; Brookhouse et al. 2008; Brookhouse and Bi 2009; Drew et al. 2013; O'Donnell et al. 2016; Nitschke et al. 2017). Despite their urban location, the Melbourne City street trees were sensitive to precipitation (*Q. robur* $r > 0.5$ and *Ulmus* spp. $R > 0.4$ winter and spring months; Nitschke et al. 2017).

Table 1. Details of tree-ring chronologies used in at least one reconstruction in the western Tasmania.

Site	Species	Chronology type	First	Last	*n*(*N*)	No. cells	% cells	+	−
BTAMFA	LGFR	MFA	1850	2009	20(14)	350	37.27		t0
*COLWRD	PHAS	LW TRD	1700	2011	44(28)	350	37.27	**t1**	
FBDRDE	ATSE	EW TRD	1685	2011	25(18)	350	37.27	t0	
*MLELM2V	ULSP	RW	1882	2012	31(17)	350	37.27		**t1**
*SWCTRW	PHAS	RW	1590	2012	151(70)	350	37.27		**t1**
*SWCRW	PHAS	RW	1590	2009	53(32)	350	37.27		**t1**
FEBTRD	ATSE	TRD	1684	2011	27(15)	349	37.17	t0	
BCHUPD	LGFR	RW	1590	2012	112(50)	348	37.06	t0	
FEBDEN	ATSE	DNS	1619	2011	30(16)	348	37.06		t0
RESLAK	ATSE	RW	1700	2008	40(17)	348	37.06	t0	
BTATRD	LGFR	TRD	1810	2009	26(14)	345	36.74		t0
FEBWTT	ATSE	WT	1619	2011	43(26)	344	36.67		
*COLWDN	PHAS	LW DNS	1700	2011	17(12)	343	36.53		t0
EASCTP	PHAS	RW	1590	2007	167(88)	314	33.44		**t1**
FEBEWW	ATSE	EWW	1600	2011	56(20)	304	32.37		**t1**
BTADNS	LGFR	DNS	1830	2009	21(14)	299	31.88	**t1**	
KBMSEW	ATSE	EWW	1650	2011	65(26)	297	31.63	t0	
KBSTRW	ATSE	RW	1590	2011	34(12)	294	31.31	t0	
BCHWTT	LGFR	WT	1600	2012	15(10	282	30.03		t0
LMHigh	LGFR	RW	1590	2011	48(24)	280	29.82	t0	
PBTDHP	LGFR	TRD	1590	2012	48(25)	277	29.5		t0
MCKWTT	ATCU	WT	1590	2009	30(20)	274	29.18		t0
PBWTHP	LGFR	WT	1590	2012	46(25)	272	29		t0
MFIELD	ATCU	RW	1590	2008	93(49)	271	28.86	t0	
*SRTRW	LGFR	RW	1590	2017	178(101)	271	28.86		t0
TPKWHP	LGFR	WT	1590	2012	33(17)	267	28.46	**t1**	t0
FBDNEW	ATSE	EW DNS	1684	2011	25(16)	261	27.83		t0
*COSWDN	PHAS	DNS	1530	2011	41(26)	257	27.37	t0	
MCKWTE	ATCU	EW WT	1590	2009	29(19)	250	26.62		t0
PBDNHP	LGFR	DNS	1590	2012	54(28)	241	25.67		t0
MRD2HP	LGFR	RW	1590	2009	289(148)	236	25.13	t0	
FBWTLW	ATSE	LW WT	1684	2011	23(14)	235	25.03		t0
*TNEDNL	PHAS	LW DNS	1693	2009	21(14)	235	25.03	t0	
*TNEDEN	PHAS	DNS	1697	2012	27(14)	232	24.71	t0, **t1**	
MCKDEN	ATCU	DNS	1590	2009	29(22)	229	24.39		t0
CMTEW	ATSE	EWW	1590	2008	43(26)	215	22.9	t0	
MCKWTL	ATCU	LW WT	1590	2009	27(18)	214	22.79		t0
*COMNDN	PHAS	DNS	1700	2011	15(9)	212	22.58	t0	
PBWHP	LGFR	RW	1590	2012	71(36)	211	22.47		**t1**

(*Continued on next page*)

Table 1. (*Continued*)

Site	Species	Chronology type	First	Last	*n*(*N*)	No. cells	% cells	+	−
PNLMCP	ATCU	RW	1590	2009	115(54)	209	22.26		**t1**
TPKTHP	LGFR	TRD	1590	2012	32(17)	203	21.62		t0, **t1**
CMTCMT	ATSE	RW	1590	2008	221(111)	202	21.51	t0	
MCKDNe	ATCU	EW DNS	1590	2009	28(16)	193	20.55		t0
FEBLWW	ATSE	LWW	1481	2011	45(21)	180	19.17		t0
BCHTRD	LGFR	TRD	1600	2012	15(10)	173	18.42		t0
*SRTWT	LGFR	WT	1590	2017	111(57)	168	17.89		t0
FBDNLW	ATSE	LW DNS	1684	2011	25(17)	137	14.59		t0
*COSWRD	PHAS	TRD	1550	2011	50(32)	136	14.48	**t1**	
*SRTTRD	LGFR	TRD	1590	2017	80(49)	122	12.99		t0, **t1**
*SRTDNS	LGFR	DNS	1590	2017	95(61)	99	10.55		t0
MSATRW	ATSE	RW	1731	2011	32(12)	99	10.54	t0	
MRDEWW	ATSE	EWW	1590	2011	39(24)	78	8.31		**t1**
MDKBRD	ATSE	TRD	1590	2012	26(16)	75	7.99	t0	
TPKDHP	LGFR	DNS	1590	2012	27(18)	74	7.89	**t1**	
MCKDNl	ATCU	LW DNS	1590	2009	28(19)	74	7.88		t0
BCHDNS	LGFR	DNS	1590	2012	15(10)	65	6.92		t0
MDKBWT	ATSE	WT	1590	2012	29(17)	65	6.92		t0
*TNETRD	PHAS	TRD	1691	2012	23(12)	43	4.58		t0
MDKBDN	ATSE	DNS	1590	2011	28(16)	40	4.26		t0
LKMACK	ATCU	RW	1590	2008	188(106)	35	3.73		**t1**
*TNERDE	PHAS	EW TRD	1698	2009	20(13)	35	3.73		t0, **t1**
*MELPOPV	POSP	RW	1882	2012	16(8)	23	2.45		**t1**
MTREAD	ATSE	RW	1590	2011	119(62)	23	2.45		**t1**
FBWTEW	ATSE	EW WT	1684	2011	24(16)	19	2.02		t0
*COMMRD	PHAS	TRD	1700	2011	21(13)	18	1.92		t0
MCKRDe	ATCU	EW TRD	1590	2009	25(17)	18	1.92	t0	
*TNEWTT	PHAS	WT	1691	2012	23(12)	18	1.92		t0, **t1**
BAWRWV	EUPA	RW	1801	2008	181(72)	9	0.96		**t1**
*TNEWTL	PHAS	LW TRD	1706	2009	22(14)	8	0.85	t0, **t1**	
*MLELMIV	ULSP	RW	1900	2012	21(14)	4	0.43		**t1**
FEBTRW	ATSE	RW	1590	2011	63(23)	3	0.32		**t1**
MRDLWW	ATSE	LWW	1590	2011	26(17)	1	0.11	t0	

* indicates location provided is approximate because chronology is a composite of two or more sites. A ^{V} denotes a Victorian tree-ring site. *n*(*N*) shows the number of samples (trees) at each site. No. cells and % cells refer to the number and percentage of grid cell reconstructions respectively for which the chronology used. Chronology order in Table is from highest to lowest % of grid cell reconstructions that utilised each chronology. The + and − columns represent the sign of correlation with the FFDI target. t0 indicates concurrent response, **t1** in bold indicates lagged response. The sign of correlation between a particular chronology for a particular lag (i.e. t0 or t1) and the target was the same for all grid cell reconstructions to which the chronology contributed. See Supplementary Table S2 for site locations and names, and Supplementary Table S3 for explanation of chronology types.

Trees sampled at Tasmanian sites were typically older individuals, although where possible, an effort was made to also sample slightly younger trees (trees estimated to be ~50–60% of the age of older trees). This effort, however, was limited by restrictions on permits issued by land management agencies.

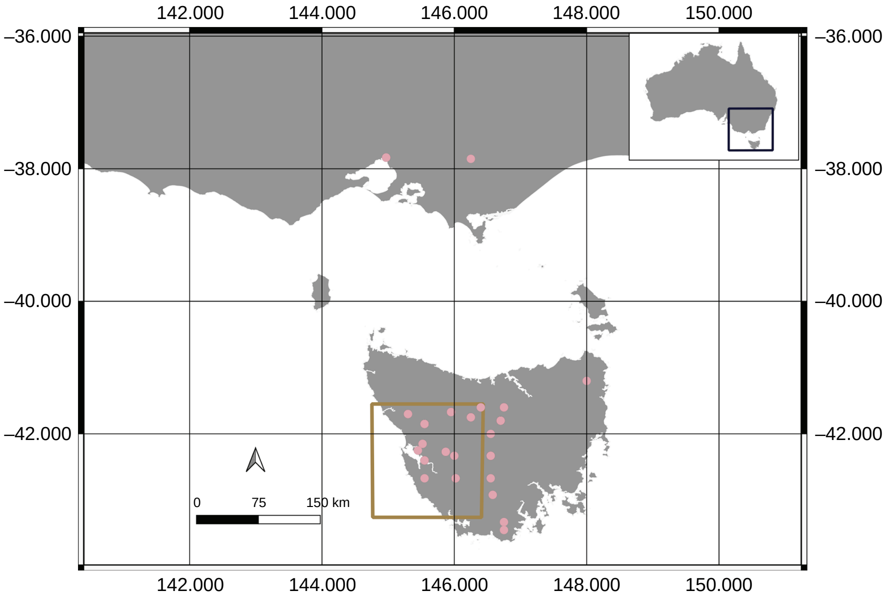

Fig. 1. Study area. Large black box in inset map shows area initially examined. Brown box over Tasmania shows the area for which reconstructions were averaged and analysed. Pink dots mark locations of tree-ring chronologies used.

In dendroclimatology, tree-ring chronologies undergo a standardisation process in an effort to minimise non-climatic variability. Standardisation method varied across sites, with a negative exponential curve or negative regression line used to standardise the five Victorian sites that were growing in relatively open conditions and exhibited this growth pattern. This standardisation method, however, was not suitable for the Tasmanian sites which typically grow in closed canopy forests and experience much higher levels of dynamic forest processes. Additionally, many of the Tasmanian chronologies were based on wood properties other than ring width, and did not display a semimonotonic negative trend in growth over time. These chronologies were standardised using either an age-dependent spline (Melvin *et al.* 2007) or the Friedman supersmoother (Friedman 1984). The stiffness of the 50% cutoff age-dependent spline varies over time, being more flexible at the start of the series (here, initial segment length was 50 years), and becoming progressively stiffer through to the modern end of the series as interannual growth variability typically declines. When using the Freidman variable span supersmoother, an α-value of 7 or 8 was used to impart moderate flexibility, while avoiding removal of too much medium-frequency variability. The α-value was determined through inspection of smoothing curves and series. Standardisation was done within the signal-free framework (Melvin and Briffa 2008), using the RCSsigFree_SingleMWRE software developed by Dr Ed Cook that extends the functionality of ARSTAN (Cook 1985). Final chronologies were computed using residuals rather than ratios, and an age-dependent spline was used to stabilise increased variance that may be due to low sample depth. All chronologies that extended to at least 2007 (many chronologies end between 2000 and 2012) were used for reconstruction purposes. Portions of chronologies with fewer than five samples were excluded from analysis.

FFDI data

The daily gridded FFDI data were sourced from the Australian Bureau of Meteorology. With growing concern over high fire-danger seasons, we focused our reconstructions on high fire-danger conditions. For the purposes of this study, we define high fire-danger days for an individual grid cell as those in the upper quartile of values for that grid cell over the January to March season. This effectively means we focus on relative values rather than imposing a fixed FFDI value across all grid cells. Using an absolute fixed value of FFDI (e.g. FFDI > 50) would result in significant spatial biases because FFDI will generally be lower in southern Tasmania than on the Australian mainland (Dowdy *et al.* 2009; and compare the approach taken by Dowdy 2018). Southern Tasmania can experience high fire-danger weather and destructive fires, even when FFDI appears low by mainland Australian standards. Average January–March FFDI for our study region, for example, is 8.2 with a range of 3.67–15.5 (January, 5–16; February, 4–16; March, 2–13). The FFDI briefly peaked at 25 in the zone of the 2019 fires in southern Tasmania when they occurred. For most of the 2-week period after fire ignitions on 15th January 2019, however, FFDI was <10 (Wardlaw 2021). Similarly, fire conditions were described as 'moderate' in the lead up to the 2016 fires on the Central Plateau in Tasmania. The highest FFDI value recorded during this fire event was 36 at the town of Cressy on the plains below The Plateau (Bureau of Meteorology 2016). To put this in context, fire weather warnings in the east Australian states are generally issued when FFDI $\geq$ 50 (severe fire danger).

We used the upper quartile in preference to more extreme values (e.g. upper decile) because these more extreme values resulted in a large number of 0s in the data set, and hence a lack of interannual variability that prohibited a useful reconstruction. This procedure enabled us to examine the possibility of producing statistically valid reconstructions of seasonal fire danger (expressed as the number of high fire-danger days) across a broad geographical area.

The reconstructions

We first investigated the potential to use the existing tree-ring chronologies to reconstruct high fire-danger seasons, as defined above, across a broad swathe of southeastern Australia (from 31.15–44°S, and 138.8–152.15°E). This enabled us to subsequently identify regions to target for further examination, and regions for which the current set of tree-ring data cannot provide useful and temporally stable reconstructions.

We began by assessing correlations between the gridded FFDI and all non-lagged and lag-1 tree-ring predictors. For each grid cell, three measures of correlation (Pearson R, Spearman R and Robust Pearson) were used to assess significance (two-tailed; $P < 0.1$) with the target FFDI.

Predictors lagged by 1 year were also used because in many cases, the Tasmanian trees use resources stored from the previous growing season, and the current year's growth is also linked to the previous year's conditions (Buckley *et al.* 1997; Allen *et al.* 2001, 2011). No weighting was applied to predictors. All statistically significant predictor chronologies were then passed to a nested principal component regression procedure (see Cook *et al.* 1999). Using this approach, one final reconstruction based on principal components of the predictors (where possible) was produced for each of the 36 566 grid cells. Nesting the principal component-based reconstructions accounts for the declining number of predictors back in time (see Table 1 for lengths of input predictors). For each grid point, successive reconstructions are produced, each successive one longer, but based on fewer predictors as they drop out. These reconstructions are then spliced together after rescaling to recover lost variance due to regression in the calibration period. Using a split calibration–verification approach common to tree-ring reconstructions, we first used the 1979–2007 period for calibration and the 1950–1978 period for verification. We then reversed these periods to check temporal stability of reconstruction quality across the domain (Fig. 1).

Reconstruction quality was assessed through a series of commonly used statistics. These included R^2 for the calibration period (CRSQ), and the cross-validated reduction of error for the calibration period estimated using a leave-one-out procedure (CVRE; Michaelsen 1987). For the verification period, R^2 for the verification period (VRSQ, but note the sign before squaring is retained, so VRSQ can be negative), the reduction of error for the verification period (VRE) and the coefficient of efficiency (VCE) were calculated. Both VRE and VCE range from $-\infty$ to 1. A positive value for either statistic indicates the reconstruction is superior to the climatology (in this case, mean number of days in the upper quartile of January–March FFDI in the instrumental data set). VRE is basically a comparison of the squared differences of the instrumental data and reconstruction with the squared differences of the instrumental data and the calibration period mean. VCE is very similar, but the comparison of the squared differences of the instrumental data and reconstruction is with the squared differences of the instrumental data and the verification period mean. Obtaining a value >0 for VCE is therefore more difficult than for VRE.

The two sets of models (early and late calibration periods) and their resultant statistics (Fig. 2) were used to identify general regions for which spatial clusters of reconstructions could be verified (based on VRE > 0) for both the 1979–2007 (late) and 1950–1978 (early) calibration periods. The exact area over which verification occurs differs for the two different calibration periods. From these models, a substantial cluster of verifying grid points for both periods was identified for western Tasmania (south of −41.5°S and west of 146.5°E; Fig. 1). Although there are patches of reconstructions in the northwest of the domain that obtain VRE > 0 (Fig. 2), there is considerable spatial instability across the two periods in relation to where those cells were located. Therefore, we did not select the northwest region for further examination.

We extracted all reconstructions in the west Tasmanian region and applied three different criteria to produce three data sets for the early and late calibration periods. The first set of reconstructions for consisted of all reconstructions in the defined region (ALL) extending back to 1590; the second, only reconstructions for which VRE > 0 (VRE0); and the third, only those grid cell reconstructions for which VCE > 0 (VCE0). We use only the period from 1590 because prior to this time, the number of skilful reconstructions (as measured by VRE and VCE) rapidly declines. The rationale for examining these three sets of reconstructions for each region is to determine whether reconstructions that fail to pass VCE or VRE still provide patterns of temporal variability that are similar to those of the higher quality reconstructions. If this is the case, then these lower quality reconstructions may still be useful for assessing general patterns of change over recent centuries, despite their inability to obtain VRE or VCE > 0.

Once this data examination was complete, we developed reconstructions calibrated against the full 1950–2007 period. We used this full period for calibration because the sharp increase in FFDI over most recent decades meant that a model calibrated on either of the shorter calibration periods did not adequately capture lower (1970–2007 calibration period) or higher (1950–2007 calibration period) values (Supplementary Fig. S1). Using the full period for calibration somewhat alleviates this issue, but its use means no data were withheld for independent verification of models.

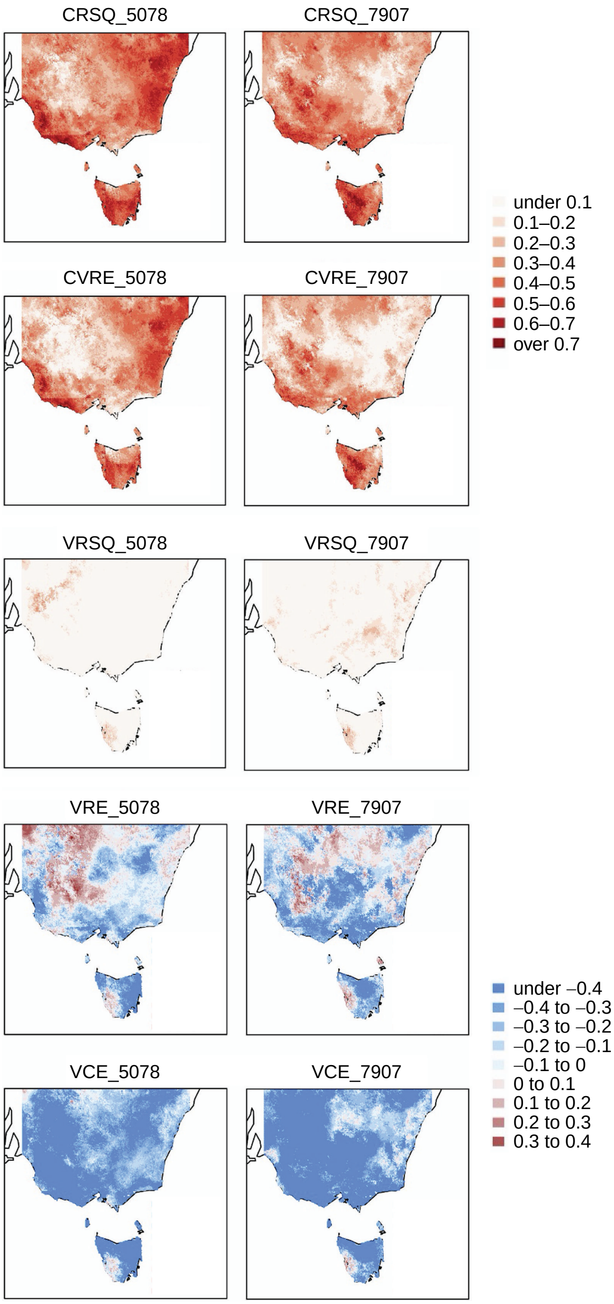

Fig. 2. Reconstruction quality statistics across whole domain initially examined for the two short calibration periods. Left: 1950–1978 calibration period, Right: 1979–2007 calibration period. CRSQ is R^2 for the calibration period, and CVRE the cross-validated reduction of error for the calibration period; VRSQ is R^2 for the verification period; VRE is the reduction of error for the verification period; and VCE is the coefficient of efficiency for the verification period.

However, we note that the area for which models were developed was initially selected based on the statistics for the two shorter calibration periods.

The FFDI reconstructions for the western Tasmanian region (Fig. 1) were averaged and a standard deviation for each year calculated. The number of grid cells used was 939.

Results

The averaged and smoothed reconstructions for the early, late and full calibration periods (see Supplementary material for more information; Supplementary Figs S1–S3) are remarkably similar to one another (Supplementary Fig. S3). Additionally, comparison of the different sets of split-period calibration models (ALL, VRE0 and VCE0) indicates that similar patterns of variability can be observed (Supplementary Fig. S4), despite the large changes in the number of cell reconstructions (Supplementary Table S1). Not unexpectedly, the visual agreement between the averaged instrumental data and the averaged full period Tasmanian reconstructions is an improvement on either of the early or late calibration period reconstructions (Fig. 3, Supplementary Fig. S1).

The average variance explained for the full period Tasmanian reconstructions is approximately 35% in the most recent nest, falling to ~25% in the earliest nest (Fig. 4). As such, the quality of the reconstructions is modest, but the positive value of VRE across much of the area for the respective early and late calibration periods (Fig. 2) indicates that the regionally averaged reconstructions exhibit useful skill (i.e. are superior to the climatology). Additionally, the positive values of CVRE (Fig. 4) indicate skill based on the full calibration period. Tree-ring chronologies used as input predictors in reconstructions are shown in Table 1 and Supplementary Tables S2, S3.

According to the averaged reconstructions (Fig. 3), although there has been a strong increase in FFDI in the past 30 years, reconstructed values as high as post-2000 values have previously occurred. The 5 years with the highest reconstructed number of high fire-danger days include 1656 (57.39), 1661 (54.89), 1890 (52.47), 1961 (53.2) and 2008 (58.91), while more extended periods of relatively high fire danger were reconstructed for the 1650s–early 1660s, 1860–1861, late 1880s–mid 1890s and since 2000 (Fig. 3). The 5 years for which reconstructed fire danger was lowest include: 1624 (9.94), 1664 (8.76), 1686 (9.4), 1849 (12.63) and 1965 (5.35). According to the reconstruction, more extended periods of low fire danger occurred in the early 1760s, the 1820s and the early 1920s. There has been a sustained trend towards summers with a higher number of days in the upper quartile of FFDI values over the past five decades that is not matched in the 430-year long record (Fig. 3*a*, *b*).

A total of 3938 predictor series were used in this study. These series were sourced from 1123 trees, with multiple types of series generated from many of these trees (e.g. at some sites a single tree yielded a ring width, average density, average tracheid radial diameter and average cell wall thickness chronologies – see Table 1). The total number of predictors available varied through time (Fig. 5), with the lowest numbers of samples and trees at the start and end of the 1590–2007 period and the highest numbers from 1850 to 1970. More specifically, the minimum number of

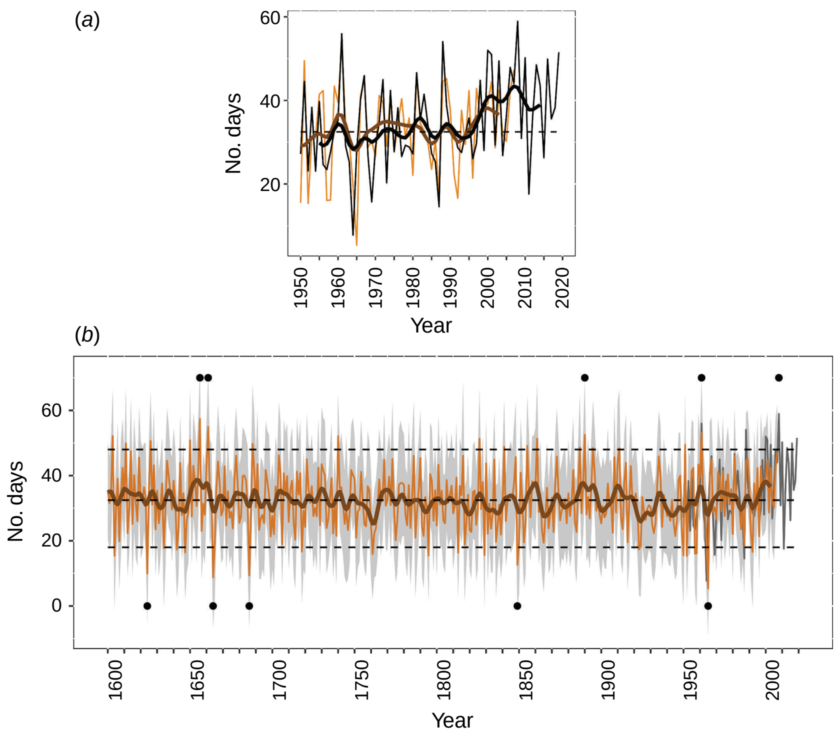

Fig. 3. The averaged reconstruction of number of days in upper quartile of FFDI values for western Tasmania. (*a*) Comparison of averaged reconstruction with instrumental data for the 1950–2007 period. Orange is reconstruction, black the instrumental period data. Thick lines are the respective smoothed data (20-year Gaussian smooth). (*b*) The average FFDI reconstruction for the 1950–2007 calibration period. Grey background shows +/− one standard deviation; thick orange line is 20-year Gaussian smooth. Dots represent the five highest and lowest fire-danger years, and values outside the dashed lines are the upper and lower 5% of fire-danger seasons based on the number of days for which local FFDI ≥ 75th percentile value. The black time series is the instrumentally based FFDI data and extends to 2019. The highest value of 58.91 high fire danger days over the 3-month window occurs in 2008. The closest reconstructed value occurs in 1656 (57.39).

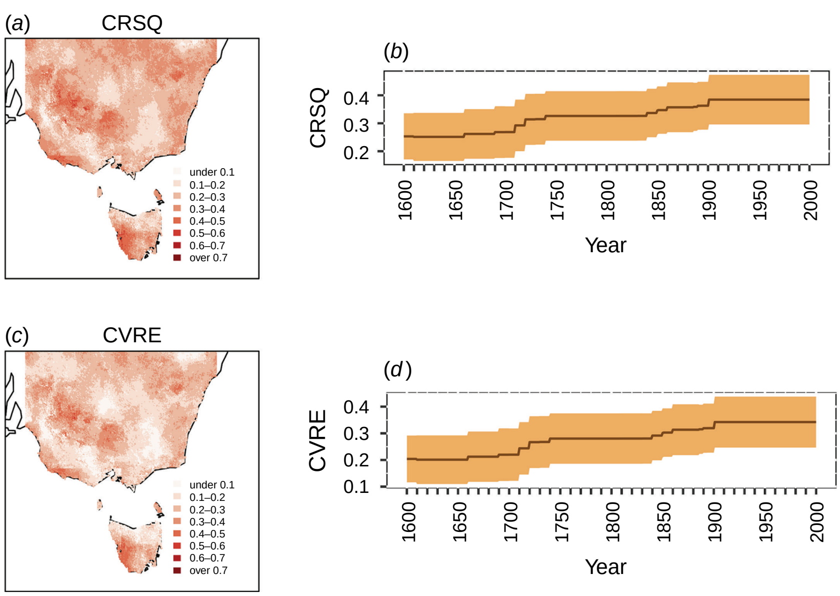

Fig. 4. (*a*) Spatial CRSQ for the 1950–2007 calibration period. (*b*) CRSQ over time. (*c*) Spatial CVRE for the 1950–2007 calibration period and (*d*) CVRE over time. Dark orange lines in (*b*) and (*d*) are the average value of CRSQ for each nest of the averaged reconstruction. Lighter orange band shows the mean ± 1σ.

predictors included for any year was 1253 samples (1590–1591), 763 trees (1590) and 457 ring-width series (1590). Maximum number of input predictors used was 2668 samples (1910, 1915), 1528 trees (1653, 1946) and 775 ring width series (1950, 1952, 1960).

The correlation of a single predictor chronology with FFDI was consistently of the same sign across all grid cell reconstructions in which it was used in the subsequent PC-regression reconstruction model (Table 1). In some cases where both lagged and non-lagged chronologies were used, the sign of correlation of lagged and non-lagged chronology differed (Table 1). The signs of these correlations with FFDI were also consistent with dominant climate relationships shown in previous work for different chronologies (Allen *et al.* in revision; Buckley *et al.* 1997; Allen *et al.* 2001, 2011, 2017*b*, 2018; Nitschke *et al.* 2017). For example, the precipitation-sensitive *Quercus* and *Ulmus* respond positively to precipitation and have a negative correlation with the FFDI (Table 1); the dominant response of PBDNHP to temperature is negative, as is its correlation

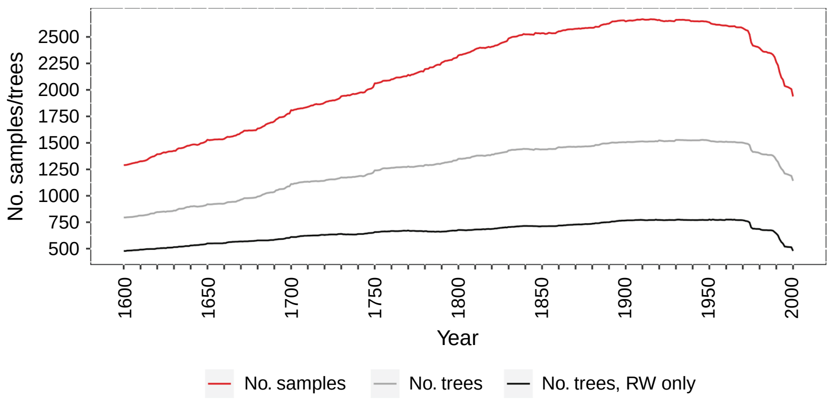

Fig. 5. Number of samples and trees available for use in reconstructions through time. Red line indicates total number of samples; green line shows the number of trees but allows duplicate trees where multiple types of chronologies were developed from them; and black shows the total number of trees available (but each tree is only counted once, regardless of the number of chronology types developed from it). There were 457 trees available in 1590 (black line) and 459 in 2007 (black line).

with the FFDI target; high elevation BCHUPD Huon pine ring width is positively associated with both temperature and the FFDI; and the dominant response of PNLMCP ring width is lagged and negative to both temperature and the FFDI (Table 1, Supplementary Tables S2, S3; Allen *et al.* 2018, in revision).

Lagarostrobos franklinii is the most commonly selected species, with *Populus alba* and *E. pauciflora* least selected (Table 2). Looking at selection based on the weighted proportion of chronologies used (Table 2) for the species (and ignoring cases where $n = 1$), the most commonly selected species were *Ulmus* spp. ($n = 2$) followed by *A. cupressoides* ($n = 10$) and then *P. aspleniifolius* ($n = 15$). With respect to chronology types, weighted values (again ignoring cases where $n = 1$) indicate that earlywood density ($n = 2$), latewood cell wall thickness ($n = 2$) and latewood tracheid radial diameter ($n = 2$) were, on average, the most selected chronology types (Table 2). In contrast, ring width chronologies ($n = 21$) were least selected based on the weighted measure. Athough these averages present some interesting information, caution should be applied to broad inferences made regarding the usefulness of chronology type or species. For example, the ring width chronologies for BCHUPD and RESLAK are selected in over 37% of grid cell reconstructions, whereas the FEBTRW chronology is utilised in less than 1% of reconstructions (Table 1).

Discussion

In a short–medium term context, Doerr and Santin 2016 found that area burnt by fire on a global basis has actually decreased, particularly over the first half of the 20th Century (Flannigan *et al.* 2009*b*), before increasing again. On a similar time scale, Abram *et al.* (2021) indicated that dangerous fire weather in southeastern Australia (not including Tasmania) has now begun to emerge from the historical background (defined as $\geq 2\sigma$ above the natural variability level for 1950–1999). Our reconstructions are consistent with these findings. Although there have been individual years in previous centuries when the reconstructed number of high fire danger days in southwest Tasmania was higher than many recent years, the persistent upward trend in the number of high fire-danger days since ~1940 is unprecedented in the 430-year context. The lack of years with a low number of high fire-danger days in western Tasmania since the 1970s is also unusual in the 430-year context (Fig. 3). Of the 23 years for which the number of high fire danger days is greater than 1σ above the mean (reconstruction period 1590–2007 plus instrumental data from 2008), seven occur in the post-1950 period (1951, 1961, 2008, 2010, 2013, 2016, 2019), while the remaining 16 are spread over the preceding 360 years (1603, 1611, 1626, 1650, 1656, 1661, 1668, 1740, 1826, 1841, 1855, 1861, 1887, 1890, 1895, 1911). By providing a long-term perspective, our reconstruction adds further weight to growing concerns about the trend towards the increasing occurrence of high fire-danger weather found in short-term instrumental records.

The skill of the FFDI reconstructions is comparable to previous hydroclimate reconstructions produced for Tasmania. The Allen *et al.* (2015) streamflow reconstructions for Tasmania have explained 23–35% of December–January streamflow and dam inflow over the period 1560–2007, and the July–August dam inflow reconstruction explained 23% of the variance. However, the skill metrics for both these reconstructions, as well as the current FFDI reconstruction, are lower than the Palmer *et al.* (2015) spatial drought reconstruction that explained more than 50% of variance in drought conditions over Tasmania. Similarly, the FFDI reconstruction skill is lower than previous temperature reconstructions for Tasmania. The Cook *et al.* (2006) warm season (November–April) reconstruction explained approximately 45% of the variability over the November–April period, with Allen *et al.* (2018) later improving this to 50–60% through the use of alternative wood properties to reconstruct December–February temperature. Recent preliminary work by Wilson *et al.* (2021) indicates that a similar level of variance (50–60%) can be explained in summer temperatures for Tasmania using chronologies developed from blue-intensity data. For the cool season (July–October), Allen *et al.* (2019) explained

Table 2. Chronologies used in reconstructions by type and species.

Chronology type	Average%	no_crns	Weighted
Average cell wall thickness	22.51	8	2.81
Average density	20.30	11	1.85
Average latewood density	25.03	1	25.03
Average microfibril angle	37.27	1	37.27
Average tracheid radial diameter	18.54	10	1.85
Earlywood cell wall thickness	14.32	2	7.16
Earlywood density	24.19	2	12.10
Earlywood tracheid radial diameter	14.31	3	4.77
Earlywood width	23.80	4	5.95
Latewood cell wall thickness	23.91	2	11.96
Latewood density	19.67	3	6.56
Latewood tracheid radial diameter	19.06	2	9.53
Latewood width	9.64	2	4.82
Ring width	20.89	21	0.99
Species	Average%	no_crns	Weighted
ATCU	18.82	10	1.88
ATSE	19.76	23	0.86
EUPA	0.96	1	0.96
LGFR	24.41	20	1.22
PHAS	19.82	15	1.32
POSP	2.45	1	2.45
ULSP	18.85	2	9.43

Second column shows the average percentage of reconstructions for which each chronology type (species) used. Third column refers to the number of chronologies (no_crns) in the predictor pool of that type or species. The weighted column is simply the quotient of the second and third columns. See Table 1 for details regarding frequency of selection of individual site chronologies.

between 25 and 50% of the variance across the far southeast of Australia. However, even though the skill of our average FFDI reconstruction is moderate, it nonetheless provides a longer-term lens for assessing variation in fire danger over the past 430 years. The consistency amongst the three different versions of averaged reconstructions, and for reconstructions calibrated on different periods (Supplementary Figs S3, S4), lends confidence to the conclusions reached here that the number of high fire danger days over the January–March period is unusual in a 430-year context, and adds to concerns based on analyses of shorter instrumental data.

The relatively moderate skill of the reconstructions is likely associated with disparate scales of temporal sensitivity between FFDI values and how a tree responds to its environment. A tree's response to a season with a high number of high fire-danger days will also be mediated by conditions leading up to the season. As discussed in Methods, and shown in Table 1, many of the Tasmanian chronologies are sensitive to conditions of the previous year. High fire-danger summer seasons following on from dry warm conditions the previous year, and/or winter–spring drought, are more likely to result in a negative impact on tree growth than if preceding conditions had been wet and mild. Therefore, the same high fire-danger conditions (January–March) in two different years may produce different responses, contributing to modest skill. Further, the tree-ring chronologies are not responding directly to the FFDI; rather their relationship with fire danger is filtered by their response to temperature and hydroclimate. Tasmania's relatively mild maritime climate also has an impact on the relatively moderate strength (compared with, for example, chronologies developed from trees close to their physiological limits) of correlations between most chronologies and climate in this region.

Our results are particularly important given the lack of fire weather indices for Australia prior to 1950. A more spatially extant tree-ring network that includes a greater range of species in locations across eastern Tasmania, and in southern Australia more broadly, may help improve the stability of reconstructions across a broader region. Sites and species with a strong response to spring and early summer may also be useful in capturing how fire danger earlier in the season has changed over recent centuries.

There are at least two important caveats associated with our study. Firstly, we have focused on the reconstruction of January–March FFDI, mainly because the strongest relationship between the predictors used and the FFDI occurred in these months. It can also be considered the core of the fire season in the southeast (Russell-Smith *et al.* 2007). This fixed season may, however, inadequately represent the fire season across the entire southeast Australian domain (Fig. 2). Use of a fixed season also means that no inferences regarding a changing season length observed in the instrumental data (Dowdy *et al.* 2009) can be made from our results. This is especially relevant because observations and modelling have shown or projected an increased length of the fire season over recent decades or into the future (Williams *et al.* 2001; Fox-Hughes *et al.* 2014; Dowdy 2018; Dowdy *et al.* 2019; Goss *et al.* 2020). The 2019–2020 bushfires, which commenced in southern Australia prior to January, illustrate this issue.

Secondly, the regionality of our results is a further consideration. Based on climate model projections, Fox-Hughes *et al.* (2014) has noted considerable variability in changing fire risk across even a small island like Tasmania. They found a lesser increase in fire danger for western compared with eastern Tasmania. They also projected an increase in the number of extreme fire weather days in spring for the southeast. These modelled regional differences may help explain why we were unable to develop higher quality reconstructions for eastern Tasmania when the majority of tree-ring sites are located in western and central Tasmania.

Our focus here has been on the possibility of reconstructing seasonal fire danger in southeastern Australia. Further work will examine the potential for developing additional tree-ring chronologies in eastern Australia beyond Tasmania. It will also examine the relationship between the fire incidence and high fire-danger seasons over recent centuries, which was beyond the scope of this paper. Information such as this will help disentangle the role of changing land management practices in altering the occurrence of fire in Australia over recent centuries, against the background of seasonal fire-danger variability.

Conclusions

Our study demonstrates that it is possible to develop modestly skilful reconstructions of past seasonal fire danger from tree-ring networks. Results for western Tasmania suggest that there is a sustained shift towards a higher number of high fire-danger days and a lower number of low fire-danger days in the summer months. The persistence of this trend is unmatched over the past 430 years, although there have been a number of years prior to instrumental records when the number of high fire-danger days was at least as high as that for the past two decades.

A more extensive tree-ring network would improve upon the useful, but modest, results obtained here. Although this study represents a first attempt to reconstruct seasonal fire danger for part of Australia, reconstructions of alternative fire indices, such as the Canadian Fire Weather Index (FWI; Van Wagner and Forest 1987), may also be fruitful where dense tree-ring networks exist.

Supplementary material

Supplementary material is available online.

References

Abram NJ, Henley BJ, Sen Gupta A, Lippman TJR, Clarke H, Dowdy AJ, Sharples JJ, Nolan RH, Zhang T, Wooster MJ, Wurtzel JB, Meissner KJ, Pitman AJ, Ukkola AM, Murphy BP, Tapper NJ, Boer MM (2021) Connections of climate change and variability to large and extreme forest fires in southeast Australia. *Nature Communications Earth and Environment* **2**, 8. doi:10.1038/s43247-020-00065-8

Allen KJ, Nichols S, Evans R, Baker P (unpublished) Characteristics of a multi-species network of conifer wood properties chronologies from southern Australia. *Dendrochronologia*. In revision.

Allen KJ, Cook ER, Francey RJ, Michael K (2001) The climatic response of *Phyllocladus aspleniifolius* (Labill.) Hook.f in Tasmania. *Journal of Biogeography* **28**, 305–316. doi:10.1046/j.1365-2699.2001.00546.x

Allen KJ, Ogden J, Buckley BM, Cook ER, Baker PJ (2011) The potential to reconstruct broadscale climate indices associated with southeast Australian droughts from *Athrotaxis* species, Tasmania. *Climate Dynamics* **37**, 1799–1821. doi:10.1007/s00382-011-1011-7

Allen KJ, Nichols SC, Evans R, Cook ER, Allie S, Carson G, Ling F, Baker PJ (2015) Preliminary December–January inflow and streamflow reconstructions from tree-rings for western Tasmania, southeastern Australia. *Water Resources Research* **51**, 5487–5503. doi:10.1002/2015WR017062

Allen KJ, Nichols SC, Evans R, Allie S, Carson G, Ling F, Cook ER, Lee G, Baker PJ (2017*a*) A 277 year cool season dam inflow reconstructions for Tasmania, southeastern Australia. *Water Resources Research* **53**, 400–414. doi:10.1002/2016WR018906

Allen KJ, Fenwick P, Palmer JG, Nichols SC, Cook ER, Buckley BM, Baker PJ (2017*b*) A 1700-year *Athrotaxis selaginoides* tree-ring width chronology from southeastern Australia. *Dendrochronologia* **45**, 90–100. doi:10.1016/j.dendro.2017.07.004

Allen KJ, Cook ER, Evans R, Francey R, Buckley BM, Palmer JG, Peterson MJ, Baker PJ (2018) Lack of cool, not warm, extremes distinguishes late 20th century climate in 979-year Tasmanian summer temperature reconstruction. *Environmental Research Letters* **13**, 034041. doi:10.1088/1748-9326/aaafd7

Allen KJ, Anchukaitis KJ, Grose MG, Lee G, Cook ER, Risbey JS, O'Kane TJ, Monselesan D, O'Grady A, Larsen S, Baker PJ (2019) Tree-ring reconstruction of cool season temperatures for far southeastern Australia, 1731–2007. *Climate Dynamics* **53**, 569–583. doi:10.1007/s00382-018-04602-2

Brookhouse MT, Bi H (2009) Elevation-dependent climate sensitivity in *Eucalyptus pauciflora* Sieb. Ex Spreng. *Trees* **23**, 1309–1320. doi:10.1007/s00468-009-0372-6

Brookhouse M, Lindesay J, Brack C (2008) The potential of tree rings in *Eucalyptus pauciflora* for climatological and hydrological reconstruction. *Geographical Research* **46**(4), 421–443. doi:10.1111/j.1745-5871.2008.00535.x

Buckley BM, Cook ER, Peterson MJ, Barbetti M (1997) A changing temperature response with elevation for *Lagarostrobos franklinii* in Tasmania, Australia. *Climatic Change* **36**, 477–498. doi:10.1023/A:1005322332230

Büntgen U, Urban O, Krusic PJ, Rybníček M, Kolář T, Kyncl T, Ač A, Koňasová E, Čáslavský J, Esper J, Wagner S, Saurer M, Tegel W, Dobrovolný P, Cherubini P, Reinig F, Trnka M (2021) Recent European drought extremes beyond common era background variability. *Nature Geoscience* **14**, 190–196. doi:10.1038/s41561-021-00698-0

Bureau of Meteorology (2016) Meteorological conditions relevant to the January 2016 Tasmanian bushfires. Commonwealth of Australia, Canberra, ACT, Australia.

Cerano-Paredes J, Iniguez JM, Villanueva-Díaz J, Vázquez-Selem L, Cervantes-Martínez R, Esquivel-Arriaga G, Franco-Ramos O, Rodríguez-Trejo DA (2021) Effects of climate on historical fire regimes (1451–2013) in *Pinus hartwegii* forests of Cofre de Perote National Park, Veracruz, Mexico. *Dendrochronologia* **65**, 125784. doi:10.1016/j.dendro.2020.125784

Chavardès RD, Daniels LD, Eskelson BNI, Pickell PD (2019) Monthly adaptations of the Drought Code reveal nuanced fire-drought associations in montane forests with a mixed severity fire regime. *International Journal of Wildland Fire* **28**, 445–455. doi:10.1071/WF18119

Chavardès RD, Daniels LD, Eskelson BNI, Gedalof Z (2020) Using complementary drought proxies improves interpretations of fire histories in montane forests. *Tree-ring Research* **76**, 74–88. doi:10.3959/TRR2019-10a

Collins KM, Price OF, Penman TD (2015) Spatial patterns of wildfire ignitions in southeastern Australia. *International Journal of Wildland Fire* **24**(8), 1098–1108. doi:10.1071/WF15054

Cook ER (1985) A time-series spproach to tree-ring dtandardisation. PhD Thesis University of Arizona, Tucson, AZ, USA.

Cook E, Bird T, Peterson M, Barbetti M, Buckley B, D'Arrigo R, Francey R, Tans P (1991) Climatic change in Tasmania inferred from a 1089-year tree-ring chronology of Huon pine. *Science* **253**, 1266–1268. doi:10.1126/science.253.5025.1266

Cook ER, Meko DM, Stahle DW, Cleaveland MK (1999) Drought reconstruction for the continental United States. *Journal of Climate* **12**, 1145–1162. doi:10.1175/1520-0442(1999)012<1145:DRFTCU>2.0.CO;2

Cook ER, Buckley BM, D'Arrigo RD, Peterson MJ (2000) Warm-season temperatures since 1600 BC reconstructed from Tasmanian tree rings and their relationship to large-scale sea surface temperature anomalies. *Climate Dynamics* **16**, 79–91. doi:10.1007/s003820050006

Cook ER, Buckley BM, Palmer JG, Fenwick P, Peterson MJ, Boswijk G, Fowler A (2006) Millennia-long tree-ring records from Tasmania and New Zealand: a basis for modelling climate variability and forcing, past, present and future. *Journal of Quaternary Science* **21**, 689–699. doi:10.1002/jqs.1071

Cook ER, Seager R, Heim RRJr, Vose RS, Herweijer C, Woodhouse C (2010) Megadroughts in North America: placing IPCC projections in a long-term palaeoclimate context. *Journal of Quaternary Science* **25**, 48–61. doi:10.1002/jqs.1303

CSIRO and Bureau of Meteorology (2015) Climate Change in Australia Technical Report. Available at https://www.climatechangeinaustralia.gov.au/en/publications-library/technical-report/

Cullen LE, Grierson PF (2009) Multi-decadal scale variability in autumn–winter rainfall in south-western Australia since 1655 AD as reconstructed from *Callitris columellaris*. *Climate Dynamics* **33**, 433–444. doi:10.1007/s00382-008-0457-8

Davey SM, Sarre A (2020) Editorial: the 2019/20 Black Summer bushfires. *Australian Forestry* **83**(2), 47–51. doi:10.1080/00049158.2020.1769899

Doerr SH, Santín C (2016) Global trends in wildfire and its impacts: perceptions versus realities in a changing world. *Philosophical Transactions of the Royal Society B: Biological Sciences* **371**, 20150345. doi:10.1098/rstb.2015.0345

Dowdy AJ (2018) Climatological variability of fire weather in Australia. *Journal of Applied Meteorology and Climatology* **57**(2), 221–234. doi:10.1175/JAMC-D-17-0167.1

Dowdy AJ, Mills GA, Finkele K, de Groot W (2009) Australian fre weather as represented by the McArthur Forest Fire Danger Index and the Canadian Forest Fire Weather Index. CAWCR Technical Report No. 10. CSIRO and the Bureau of Meteorology, Canberra, ACT, Australia.

Dowdy AJ, Ye H, Pepler A, Thatcher M, Osbrough SL, Evans JP, Di Virgilio G, McCarthy N (2019) Future changes in extreme weather and pyroconvection risk factors for Australian wildfires. *Scientific Reports* **9**(1), 10073. doi:10.1038/s41598-019-46362-x

Drew DM, Allen K, Downes GM, Evans R, Battaglia M, Baker P (2013) Wood properties in a long-lived conifer reveal strong climate signals where ring-width series do not. *Tree Physiology* **33**, 37–47. doi:10.1093/treephys/tps111

Esper J, St George S, Anchukaitis K, D'Arrigo R, Ljungqvist FC, Luterbacher J, Schneider L, Stoffel M, Wilson R, Büntgen U (2018) Large-scale millennial-length temperature reconstructions from tree-rings. *Dendrochronologia* **50**, 80–90. doi:10.1016/j.dendro.2018.06.001

Flannigan M, Stocks B, Turetsky M, Wotton M (2009*a*) Impacts of climate change on fire activity and fire management in the circumboreal forest. *Global Change Biology* **15**, 549–560. doi:10.1111/j.1365-2486.2008.01660.x

Flannigan MD, Krawchuk MA, de Groot WJ, Wotton BM, Gowman LM (2009*b*) Implications of changing climate for global wildland fire. *International Journal of Wildland Fire* **18**, 483–507. doi:10.1071/WF08187

Fletcher M-S, Hall T, Alexandra AN (2020) The of an Indigenous constructed landscape following British invasion of Australia: an insight into the deep human imprint on the Australian landscape. *Ambio* **50**, 138–149. doi:10.1007/s13280-020-01339-3

Fox-Hughes P, Harris R, Lee G, Grose M, Bindoff N (2014) Future fire danger climatology for Tasmania, Australia, using a dynamically downscaled regional climate model. *International Journal of Wildland Fire* **23**, 309–321. doi:10.1071/WF13126

Friedman JH (1984) A variable span scatterplot smoother. Technical Report No. 5. Laboratory for Computational Statistics, Stanford University, Stanford, CA, USA.

Goss M, Swain DL, Abatzoglou JT, Sarhadi A, Kolden CA, Williams AP, Diffenbaugh NS (2020) Climate change is increasing the likelihood of extreme autumn wildfire conditions across California. *Environmental Research Letters* **15**, 094016. doi:10.1088/1748-9326/ab83a7

Hanson CT, Sherriff RL, Hutto RL, DellaSalla DA, Veblen TT, Baker WL (2015) Chapter 1 – Setting the stage for mixed- and high-severity fires. In 'The Ecological Importance of Mixed-Severity Fires: Nature's Phoenix'. (Eds DA DellaSala, CT Hanson) pp. 3–22. (Elsevier: Waltham, MA, USA)

Harris S, Lucas C (2019) Understanding the variability of Australian fire weather between 1973 and 2017. *PLoS One* **14**(9), e0222328. doi:10.1371/journal.pone.0222328

Hessl AE, Ariya U, Brown P, Byambasuren O, Green T, Jacoby G, Sutherland EK, Nachin B, Maxwell S, Pederson N, De Grandpré L, Saladyga T, Tardif JC (2011) Reconstructing fire history in central Mongolia from tree-rings. *International Journal of Wildland Fire* **21**(1), 86–92. doi:10.1071/WF10108

Holz A, Paritsis J, Mundo IA, Veblen TT, Kitzberger T, Williamson GJ, Aràoz E, Bustos-Schindler C, Gonzàlez ME, Grau HR, Quezada JM (2017) Southern annular mode drives multicentury wildfire in southern South America. *Proceedings of the National Academy of Sciences* **114**, 9552–9557. doi:10.1073/pnas.1705168114

Ivanova GA, Ivanov VA, Kukavskaya EA, Soja AJ (2010) The frequency of forest fires in Scots pine stands of Tuva, Russia. *Environmental Research Letters* **5**(1), 015002. doi:10.1088/1748-9326/5/1/015002

Jones DA, Wang W, Fawcett R (2009) High-quality spatial climate datasets for Australia. *Australian Meteorological and Oceanographic Journal* **58**(4), 233. doi:10.22499/2.5804.003

Keetch JJ, Byram GM (1968) A drought index for forest fire control. Research paper SE-38. USDA Forest Service, Southeastern Forest Experiment Station 35. Asheville, SC, USA

Kharuk VI, Dvinskaya ML, Petrov IA, Im ST, Ranson KJ (2016) Larch forests of middle Siberia: long-term trends in fire return intervals. *Regional Environmental Change* **16**(8), 2389–2397. doi:10.1007/s10113-016-0964-9

Li J, *et al.* (2013) El Niño modulation over the past seven centuries. *Nature Climate Change* doi:10.1038/NCLIMATE1936

Littell JS, Peterson DL, Riley KL, Liu Y, Luce CH (2016) A review of the relationships between drought and forest fire in the United States. *Global Change Biology* **22**, 2353–2369. doi:10.1111/gcb.13275

Mariani M, Fletcher M-S (2016) The Southern Annular Mode determined interannual and centennial-scale fire activity in southwest Tasmania, Australia. *Geophysical Research Letters* **43**, 1702–1709. doi:10.1002/2016GL068082

Marsden-Smedley JB (1998) Changes in southwestern Tasmanian fire regimes since the early 1800s. *Papers and Proceedings of the Royal Society of Tasmania* **132**, 15–29. doi:10.26749/rstpp.132.15

McArthur AG (1967) Fire behaviour in *Eucalyptus* forests. Department of National Development Forestry and Timber Bureau, Canberra, ACT, Australia.

Melvin TM, Briffa KR (2008) A "signal-free" approach to dendroclimatic standardisation. *Dendrochronologia* **26**, 71–86. doi:10.1016/j.dendro.2007.12.001

Melvin TM, Briffa KR, Nicolussi K, Grabner M (2007) Time-varying-response smoothing. *Dendrochronologia* **25**, 65–69. doi:10.1016/j.dendro.2007.01.004

Meyn A, Taylor SW, Flannigan MD, Thonicke K, Cramer W (2010) Relationship between fire, climate oscillations, and drought in British Columbia, Canada, 1920–2000. *Global Change Biology* **16**, 977–989. doi:10.1111/j.1365-2486.2009.02061.x

Michaelsen J (1987) Cross-validation in statistics climate forecast models. *Journal of Climatology and Applied Meteorology* **26**, 1589–1600. doi:10.1175/1520-0450(1987)026<1589:CVISCF>2.0.CO;2

Mooney SD, Harrison SP, Bartlein PJ, Daniau A-L, Stevenson J, Brownlie KC, Buckman S, Cupper M, Luly J, Black M, Colhoun E, D'Cotsa D, Dodson J, Haberle S, Hope GS, Kershaw P, Kenyon C, McKenzie M, Williams N (2011) Late quaternary fire regimes of Australasia. *Quaternary Science Reviews* **30**, 28–46. doi:10.1016/j.quascirev.2010.10.010

Morales M, *et al.* (2020) Six hundred years of South American tree rings reveals an increase in severe hydroclimatic events since mid-20th Century. *Proceedings of the National Academy of Sciences* **117**, 16816–16823. doi:10.1073/pnas.2002411117

Nitschke CR, Nichols S, Allen K, Dobbs C, Livesley SJ, Baker PJ, Lynch Y (2017) The influence of climate and drought on urban tree growth in southeast Australia and the implications for future growth under climate change. *Landscape and Urban Planning* **167**, 275–287. doi:10.1016/j.landurbplan.2017.06.012

Noble IR, Gill AM, Bary GAV (1980) McArthur's fire danger meters expressed as equations. *Australian Journal of Ecology* **5**, 201–203. doi:10.1111/j.1442-9993.1980.tb01243.x

O'Donnell AJ, Allen KJ, Evans RM, Cook ER, Trouet V, Baker PJ (2016) Wood density provides new opportunities for reconstructing past temperature variability from southeastern Australian trees. *Global and Planetary Change* **141**, 1–11. doi:10.1016/j.gloplacha.2016.03.010

O'Donnell AJ, Cook ER, Palmer JG, Turney CSM, Grierson PF (2018) Potential for tree rings to reveal spatial patterns of past drought variability across western Australia. *Environmental Research Letters* **13**, 024020. doi:10.1088/1748-9326/aaa204

Palmer JG, Cook ER, Turney CSM, Allen K, Fenwick P, Cook BI, O'Donnell A, Lough J, Grierson P, Baker P (2015) Drought variability in the eastern Australia and New Zealand summer drought atlas (ANZDA, CE 1500-2012) modulated by the Interdecadal Pacific Oscillation. *Environmental Research Letters* **10**, 124002. doi:10.1088/1748-9326/10/12/124002

Power MJ, *et al.* (2008) Changes in fire regimes since the last glacial maximum: an assessment based on a global synthesis and analysis of charcoal data. *Climate Dynamics* **30**, 887–907. doi:10.1007/s00382-007-0334-x

Pyne SJ (2016) Fire in the mind: changing understandings of fire in western civilization. *Philosophical Transactions of the Royal Society B: Biological Sciences* **371**, 20150166. doi:10.1098/rstb.2015.0166

Reisinger A, Ktiching RL, Hughes L, Newton PCD, Schuster SS, Tait A, Whetton P (2014) Australasia. In 'AR5 Climate Change 2014: Impacts, Adaptation, and Vulnerability. Part B: Regional Aspects'. Contribution of Working Group II to the Fifth Assessment Report of the Intergovernmental panel on Climate Change. Available at https://www.ipcc.ch/report/ar5/wg2/

Russell-Smith J, Yates CP, Whitehead PJ, Smith R, Craig R, Allan GE, Thackway R, Frakes I, Cridland S, Meyer MC, Gill AM (2007) Bushfires 'down under': patterns and implications of contemporary Australian landscape burning. *International Journal of Wildland Fire* **16**(4), 361–377. doi:10.1071/WF07018

Stahle LN, Whitlock C, Haberle SG (2016) A 17,000-year-long record of vegetation and fire from Cradle Mountain National Park, Tasmania. *Frontiers in Ecology and Evolution* **4**, 82. doi:10.3389/fevo.2016.00082

Sun C, Liu Y, Li Q, Song H, Cai Q, Fang C, Liu R, Ren Y (2021) Tree rings reveals the impacts of the Northern Hemisphere temperature on precipitation reduction in the low latitudes of east Asian since 1259 CE. *Journal of Geophysical Research Atmospheres* **126**, e2020JD033603. doi:10.1029/2020JD033603

Swetnam TW (1993) Fire history and climate change in giant *Sequoia* groves. *Science* **262**, 885–889. doi:10.1126/science.262.5135.885

Trouet V, Taylor AH, Carleton AM, Skinner CN (2006) Fire-climate interactions in forests of the American Pacific coast. *Geophysical Research Letters* **33**, 1–5. doi:10.1029/2006GL027502

van Oldenborgh GJ, Krikken F, Lewis S, Leach NJ, Lehner F, Saunders KR, van Weele M, Haustein K, Li S, Wallom D, Sparrow S, Arrighi J, Singh RK, van Aalst MK, Philip SY, Vautard R, Otto FEL (2021) Attribution of the Australian bushfire risk to anthropogenic climate change. *Natural Hazards Earth Systems Science* **21**, 941–960. doi:10.5194/nhess-21-941-2021

Van Wagner CE, Forest P (1987) Development and structure of the Canadian forest fire weather index system. Forestry Technical Report 35. Canadian Forest Service, Petawawa National Forestry Institute, Chalk River, ON, Canada.

von Platen J, Kirkpatrick JB, Allen KJ (2011) Fire frequency variation in south-eastern Tasmanian dry eucalypt forest 174–2004 from fire scars. *Australian Forestry* **74**(3), 180–189. doi:10.1080/00049158.2011.10676361

Wardlaw T (2021) Measuring a fire. The story of the January 2019 fire told from measurements at the Warra Supersite, Tasmania. *Fire* **4**, 15. doi:10.3390/fire4020015

Whitlock C, DellaSalla DA, Wolf S, Hanson CT (2015) Chapter 9 – Climate change: uncertainties, shifting baselines, and fire management. In 'The Ecological Importance of Mixed-Severity Fires: Nature's Phoenix'. (Eds DA DellaSala, CT Hanson) pp. 265–289. (Elsevier: Waltham, MA, USA)

Williams AAJ, Karoly DJ, Tapper N (2001) The sensitivity of Australian fire danger to climate change. *Climatic Change* **49**, 171–191. doi:10.1023/ A:1010706116176

Williams AP, Allen CD, Macalady AK, Griffin D, Woodhouse CA, Meko DM, Swetnam TW, Rauscher SA, Seager R, Grissino-Mayer HD, Dean JS, Cook ER, Gangodagamage C, Cai M, McDowell NG (2012) Temperature as a potent driver of regional forest drought stress and tree mortality. *Nature Climate Change* **3**, 292–297. doi:10.1038/nclimate1693

Williams AP, Seager R, Berkelhammer M, Macalady AK, Crimmins MA, Swetnam TW, Trugman AT, Buenning N, Hryniw N, McDowell NG, Noone D, Mora CI, Rahn T (2014) Causes and implications of extreme moisture demands during the record-breaking 2011 wildfire season in the southwestern United States. *Journal of Applied Meteorology and Climatology* **53**(12), 2671–2684. doi:10.1175/JAMC-D-14-0053.1

Wilson R, Allen K, Baker P, Boswijk G, Buckley B, Cook E, D'Arrigo R, Druckenbrod D, Fowler A, Grandjean M, Krusic P, Palmer J (2021) Evaluating the dendroclimatological potential of blue intensity on multiple conifer species from Tasmania and New Zealand. *Biogeosciences* **18**, 6393–6421. doi:10.5194/bg-18-6393-2021

Data availability. The gridded FFDI data are available from the Australian Bureau of Meteorology. Tree-ring chronologies used in this manuscript are available from the International Tree-Ring Databank (ITRDB) or from Craig Nitschke at the University of Melbourne (Melbourne Street Trees).

Conflicts of interest. The authors declare no conflicts of interest.

Declaration of funding. KA was supported by FT200100102 and also by DP120104322 awarded to PB.

Acknowledgements. We thank three anonymous internal reviewers from CSIRO and the Australian Bureau of Meteorology for their comments on an early version of this manuscript. We also thank three anonymous reviewers whose comments have helped to significantly improve this manuscript.

Author affiliations

[A]Geography, Planning, Spatial Sciences, University of Tasmania, Sandy Bay, Tas. 7005, Australia.

[B]School of Ecosystem and Forest Sciences, University of Melbourne, Richmond, Vic. 3121, Australia.

[C]Centre of Excellence for Australian Biodiversity and Heritage, University of New South Wales, NSW 2052, Australia.

[D]Land and Water CSIRO, Sandy Bay, Tas. 7005, Australia.

[E]Oceans and Atmosphere CSIRO, Battery Point, Tas. 7004, Australia.

[F]Australian Bureau of Meteorology, Hobart, Tas. 7000, Australia.

[G]Fenner School of Environment and Society, Australia National University, ACT 0200, Australia.

[H]Acacia Hills, Tas. 7306, Australia.